

DOI: 10.1002/adma.200800830

Converting Metallic Single-Walled Carbon Nanotubes into Semiconductors by Boron/Nitrogen Co-Doping**

By Zhi Xu, Wengang Lu, Wenlong Wang, Changzhi Gu, Kaihui Liu, Xuedong Bai,*
Enge Wang,* and Hongjie Dai

Although single-walled carbon nanotubes (C-SWNTs) that act as semiconducting molecular wires have shown promise for future versatile high-performance electronic devices,^[1–3] the coexistence of metallic and semiconducting C-SWNTs in the as-grown materials has made it notoriously difficult to scale up fabrication of carbon nanotube field-effect transistors (FETs). Recently, much effort has been devoted to the preferential growth of semiconducting versus metallic nanotubes,^[4] or to enable the facile separation of the two types of nanotube, or to selectively etch and thus remove metallic C-SWNTs.^[5–7] Thus far, it is still a challenge to realize structurally controlled growth, while post-separation and etching treatments increase the complication in application of the C-SWNTs. For large-scale fabrication of nanotube electronic devices, much remains to be done to achieve a full semiconductor by any synthesis method.

Studies on B and/or N substitutionally doped multi-walled carbon nanotubes have shown that their electronic properties mainly depend on composition.^[8–11] Doping by either B or N alone tends to produce metallic behavior.^[10,11] Theoretical calculations predict that the BCN-SWNTs possess a bandgap that is adjustable by chemical composition and atomic configuration,^[12–14] which has aroused interest in the synthesis of the ternary system of BCN-SWNTs. An early study on BCN-SWNT growth was reported by using a substitution reaction of pristine C-SWNTs.^[15] Very recently, we have realized the direct synthesis of BCN-SWNTs by chemical vapor deposition.^[16]

Herein, we report the fabrication of field-effect transistor (FET) devices using the as-prepared BCN-SWNTs. Electronic transport measurements elucidate that the BCN-SWNTs are purely semiconducting. *Ab initio* calculations indicate that the electronic structure of a C-SWNT evolves from metallic to semiconducting as a result of B/N co-doping.

The synthesis of single-walled BCN nanotubes was achieved by a plasma-assisted hot-filament chemical vapor deposition (HFCVD) method. A transmission electron microscopy (TEM) image in Figure 1a shows that the as-grown BCN-SWNTs have an integrated tubular structure with clean and smooth surfaces. Electron energy loss spectroscopy (EELS) (Fig. 1b) demonstrates the sharply defined π^* and σ^* fine structure features of the K-edges, which are characteristic of well-graphitized sp^2 -bonded hexagonal networks.^[17] By systematically quantifying the chemical compositions from EELS spectra, it is found that the nanotubes typically contain 3–8 at % of B and 5–8 at % of N. The B and N contents are about equivalent in most of the BCN-SWNTs. Importantly, in our growth experiments, we found that using either a B or N doping source alone always produced pure C-SWNT product rather than B or N doped nanotubes. This indicates that while B and N alone are difficult to dope into the C-SWNT lattice, B and N are likely to co-dope into a C-SWNT by substitution of a pair of carbon atoms, which results in B/N existing as neighboring atomic pairs in the co-doped SWNT structures. A schematic illustration of the atom configuration in a BCN-SWNT is displayed in Figure 1c, in which the atomic concentration of B/N co-doping is set as 6.25%, equivalent to that of the overall grown nanotubes.

The electronic properties of the BCN-SWNTs have been measured by fabricating their field-effect transistors (FETs). The transport measurements were carried out after annealing the samples under vacuum. Figure 2a is a typical gate-dependent transport curve of BCN-SWNTs, which shows that the on and off current ratio reaches to six orders of magnitude ($I_{\text{on}}/I_{\text{off}} = 10^6$) by a sweeping gate voltage. The device exhibits a hole-carrier depletion (Fig. 2b), i.e., the BCN nanotube is a p-type semiconductor. Ti/Au are used as electrodes, from which holes are introduced.

FET devices were first fabricated with an individual BCN-SWNT or several BCN-SWNTs bridging the electrodes. The results demonstrated that, for the 58 devices fabricated on 12 chips, 56 of them were found to be depletable (hereafter defined as $I_{\text{on}}/I_{\text{off}} > 10^3$). These devices were then examined by atomic force microscopy (AFM) to observe how many nanotubes were in the channel. Except for eight, all were single-nanotube devices. By carefully checking, there were still 20 nanotubes in these eight devices, and there were two nanotubes in the two non-depletable devices (defined as $I_{\text{on}}/I_{\text{off}} < 10^3$). Therefore, in this step, we found 68 semiconducting nanotubes out of a total of 60, which corresponds with a high percentage of 97.1% semiconducting nanotubes.

[*] Prof. X. D. Bai, Prof. E. G. Wang, Z. Xu, W. G. Lu, W. L. Wang, C. Z. Gu, K. H. Liu
Beijing National Laboratory for Condensed Matter Physics
Institute of Physics, Chinese Academy of Sciences
Beijing 100190 (P. R. China)
E-mail: xdbai@aphy.iphy.ac.cn; egwang@aphy.iphy.ac.cn
Prof. H. Dai
Department of Chemistry and Laboratory for Advanced Materials
Stanford University, Stanford, CA 94305 (USA)

[**] This work is supported by the NSF (Nos. 50725209 and 60621091), MOST (Nos. 2007CB936203, 2007AA03Z353 and 2006AA03Z402), and CAS of China. Supporting Information is available online from Wiley InterScience or from the author.

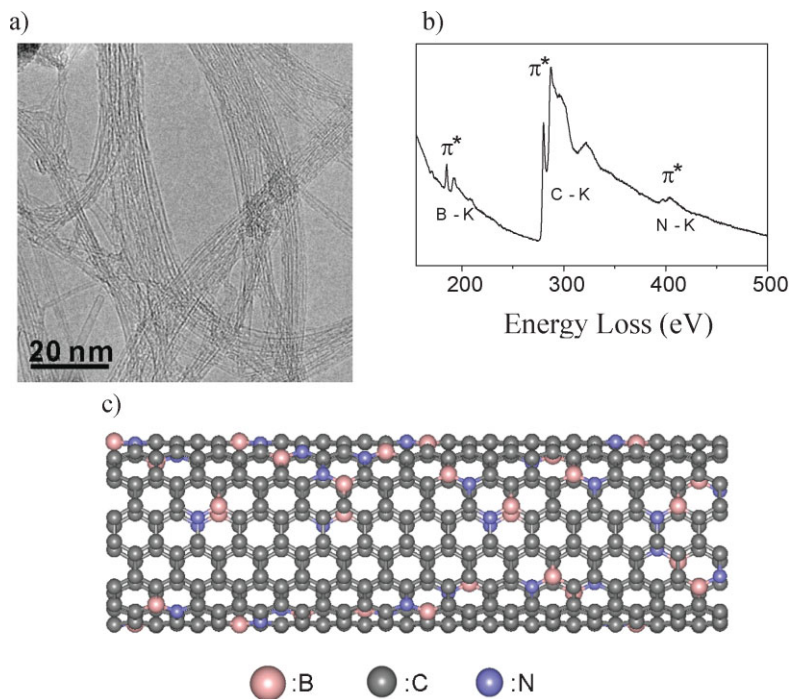


Figure 1. Structural characterization of the BCN-SWNT products. a) A typical TEM image of the as-grown BCN-SWNTs. Bundles of BCN-SWNTs with clean and straight tube walls are apparently shown to reveal the high quality of the as-grown nanotubes. b) A typical EELS spectrum taken from a BCN-SWNT bundle. c) Schematic structure of a BCN-SWCNT with a B/N doping concentration of about 6.25%, as obtained in the synthesized nanotubes.

In devices where there are more than one nanotube bridging the channel, a cutting and counting method is a very efficient way to count the nanotubes in one device.^[18] If this device is depletable, it means all nanotubes in this device are semiconducting. So a negative gate voltage can turn on all semiconducting nanotubes. The source/drain (S/D) bias is then increased to induce the electrical breakdown of these nanotubes one by one, until the S/D current drops to zero. If the device is non-depletable at first, the positive gate voltage is applied and one metallic nanotube is cut. If the device still does not become depletable, another metallic nanotube is cut. The process is repeated until all the metallic nanotubes are cut. Finally, when the device becomes depletable, the remaining semiconducting nanotubes are cut and counted. Figure 2c is a scanning electron microscopy (SEM) image that shows a multi-nanotube device (Fig. 2c), where there are eight nanotubes bridging the S/D electrodes. Figure 2d is the enlarged image of the local area marked in Figure 2c. Compared with the single-nanotube FET device, the multi-nanotube device carries a higher on current (Fig. 2e). An electrical breakdown test also confirmed that there were eight nanotubes acting as the conducting channel (Fig. 2f). Since this device is depletable, it means all of the eight nanotubes are semiconducting. In our experiments, there were still a few percent of metallic tubes in the as-grown materials, which cause some multi-nanotube transistors to be non-depletable.

By the cutting and counting method, we examined 30 multi-nanotube devices: 133 nanotubes out of 136 were found to be semiconducting. The percentage of semiconducting nanotubes was 97.8%, which is in agreement with the result by the method of single-nanotube device fabrication.

In the present study, a plasma-assisted HFCVD method is applied to grow B/N co-doped single-walled carbon nanotubes, so the possibility of selective etching of a gas-phase plasma hydrocarbonation reaction^[7,19,20] on metallic nanotubes has to be considered. Systematic plasma-assisted HFCVD experiments were carried out to synthesize C-SWNTs by using H₂ and CH₄ as reactant gases (C-SWNT I) and also by using CH₄ and B₂H₆ as reactant gases (C-SWNT II), respectively. B₂H₆ is very easy to decompose and releases H ions in plasma, thus, neutral and positive ions of H and CH₃ species, which are active to the metallic nanotubes,^[7] exist in the above two CVD environments. We carefully examined the percentage of semiconducting nanotubes among the as-grown C-SWNTs by the cutting and counting method. About 72.2% (out of 54) and 66.4% (out of 113) of the measured nanotubes were found to be depletable for the C-SWNT I and C-SWNT II, respectively (Fig. 3). The percentages of semiconducting nanotubes are very close to the theoretical prediction of two-thirds in all C-SWNTs.

For comparison, the statistical results of the BCN-SWNT, C-SWNT I, and C-SWNT II samples are demonstrated in Figure 3, which clearly shows that the selective etching can be ruled out in the growth of BCN-SWNTs.

To understand the origin of the semiconducting property of B/N co-doped C-SWNTs, we have performed *ab initio* calculations of their band structures. The VASP package along with an ultra-soft pseudo-potential (US-PP) for the ion–electron interactions and the generalized gradient approximation (GGA) for electron exchange and correlation^[21] were used. A cut-off energy for the plane wave basis of 350 eV was employed. All atomic structures of the various SWNTs considered were fully relaxed to an accuracy where the total energy difference between two ionic steps was smaller than 1 meV.

As observed in the experiments, the boron or nitride dopants are at the same concentration in the range from 3 to 8%. First, we searched various co-doped structures with B and N at adjacent sites and widely separated. It is found that B and N atoms have a strong preference to neighbor each other. The total energy with an adjacent B/N atom pair in the unit cell is about 2.0–2.6 eV lower than those with separately doped B and N atoms at different positions. This lends support to the experimental observation of B and N co-doping. We then adopted this model in band structure calculations according to the experimental results.

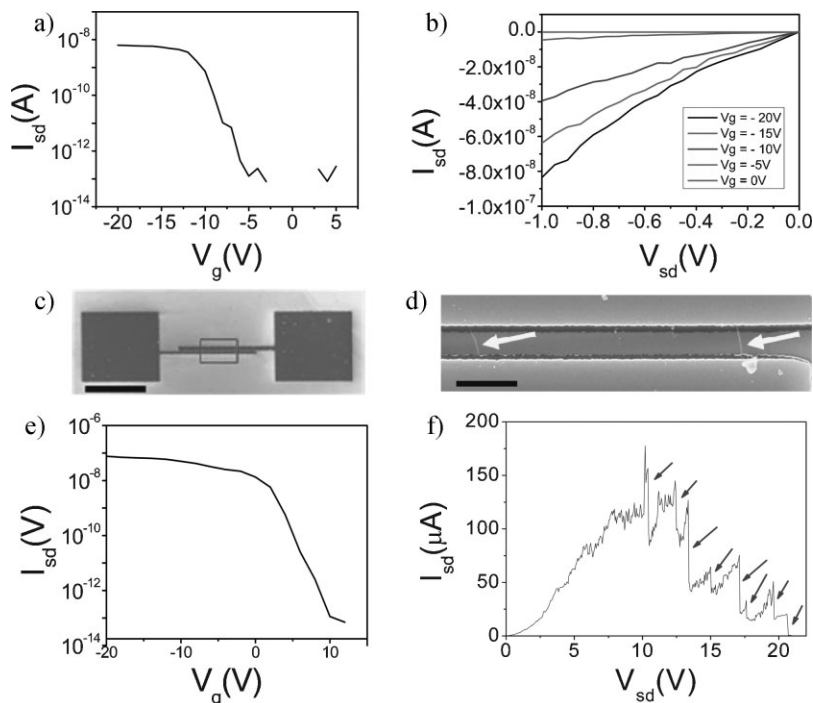


Figure 2. Characteristics of BCN-SWNT-based FET devices. a) Current (I_{sd}) vs. gate voltage (V_g) for the device, recorded under a bias of $V_{sd} = 100$ mV. The on/off ratio reaches 10^5 . Inset: AFM image of a single-tube device, which shows a BCN-SWNT diameter of ~ 1.1 nm and a channel spacing of ~ 400 nm. b) The device current I_{sd} vs. V_{sd} for various V_g . The curves were recorded by sweeping gate voltages from $V_g = -20$ to 0 V at a step of 5 V. c) SEM image of a multi-tube device. The channel is magnified in (d), and two nanotubes in the magnified area can be seen. There are eight tubes bridging the whole channel in this device. Scale bar: $50 \mu\text{m}$ in (c), $1 \mu\text{m}$ in (d). e) I_{sd} vs. V_g for the multi-tube device shows an on/off ratio $> 10^6$ and on current near 100 nA at $V_{sd} = 100$ mV. f) I_{sd} vs. V_{sd} shows sequential electrical breakdown of the tubes in the chip of (e). Eight abrupt current drops indicate that there are eight semiconducting nanotubes in the channel.

A typical metallic (5,5) C-SWNT was first employed, which has no energy gap at the Fermi level (Fig. 4a). One B/N atom pair was used to substitute two adjacent carbon atoms in a unit cell of a (5,5) C-SWNT (Fig. 4b, top), which corresponds to a B or N component ratio of 5%. The band structure of this B/N co-doped C-SWNT shows that a small energy gap of about

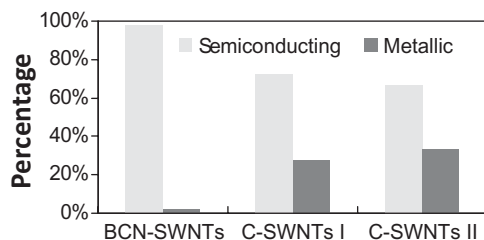


Figure 3. Histogram of the number of the semiconducting and metallic nanotubes in as-grown BCN-SWNT, C-SWNT I (using H_2 and CH_4 as reactant gases), and C-SWNT II (using B_2H_6 and CH_4 as reactant gases) samples, respectively. The percentages of the semiconducting nanotubes in the three types of the samples are 97.6, 72.2, and 66.4%, respectively.

0.1 eV opens at the Fermi level (Fig. 4b, inset). Next, another adjacent B/N atom pair is added to each unit cell. The two adjacent B/N atom pairs are separated by six carbon atoms, which corresponds to 10% of B and N (Fig. 4c, top). The energy gap is widened to about 0.5 eV (Fig. 4c). Finally, the band structure of a BN-SWNT without carbon atoms is plotted in Figure 4d, which has a quite wide gap of 4.6 eV. The *ab initio* study clearly reveals a transition of electronic property from metallic to semiconducting after B/N co-doping into C-SWNTs.

We have calculated the electronic structures of other metallic C-SWNTs at different B/N co-doping levels. For example, the (8,8) BCN-SWNT with a 6.25% B/N co-doping has an energy gap of about 0.1 eV. All of our calculations for the B/N co-doped C-SWNTs show a similar transition behavior from metallic to semiconducting, independent of the chiralities of the nanotubes although the opened gaps are different from each other. Our results clearly show that the gap opening is quite sensitive to B/N components. A band gap widens monotonically with the increase of concentration of B/N co-doping. The detailed geometry of the B/N atomic pairs may change the width of the gap slightly, but all results do not change the trend. At high doping concentrations, energy gaps are wide and no nanotubes remain metallic, but at low doping concentrations ($< 1\%$), the energy bands open small gaps. The concentration of the doped B/N atom pairs may fluctuate along the synthesized nanotube. The high doping parts have wider energy gaps and the low doping parts have lower energy

gaps. However, overall the nanotube still exhibits semiconducting characteristics. Although variations in doping concentration along the nanotube may introduce scattering, in the meantime, those BCN-SWNTs with prototypes of semiconducting C-SWNTs do not change their conductive properties and remain semiconducting. As to those rare non-depletable nanotubes, they are most probably the BCN-SWNTs with very small B/N components, because of the unavoidable doping fluctuation in growth.

Our present work focuses on the effect of B/N co-doping on the modification of the electronic structure of C-SWNTs. A study of large numbers of BCN-SWNT-based FETs indicates that the metallic C-SWNTs can be converted into semiconductors by their B/N co-doping, which aims at a scalable fabrication of nanotube electronic devices, regardless of the difficulty of the coexistence of metallic and semiconducting nanotubes in raw materials. Systematic experimental data and theoretical calculations suggest the B/N co-doped C-SWNTs possess a semiconductor nature, which could open a route to large-scale integrated nanotube electronics.

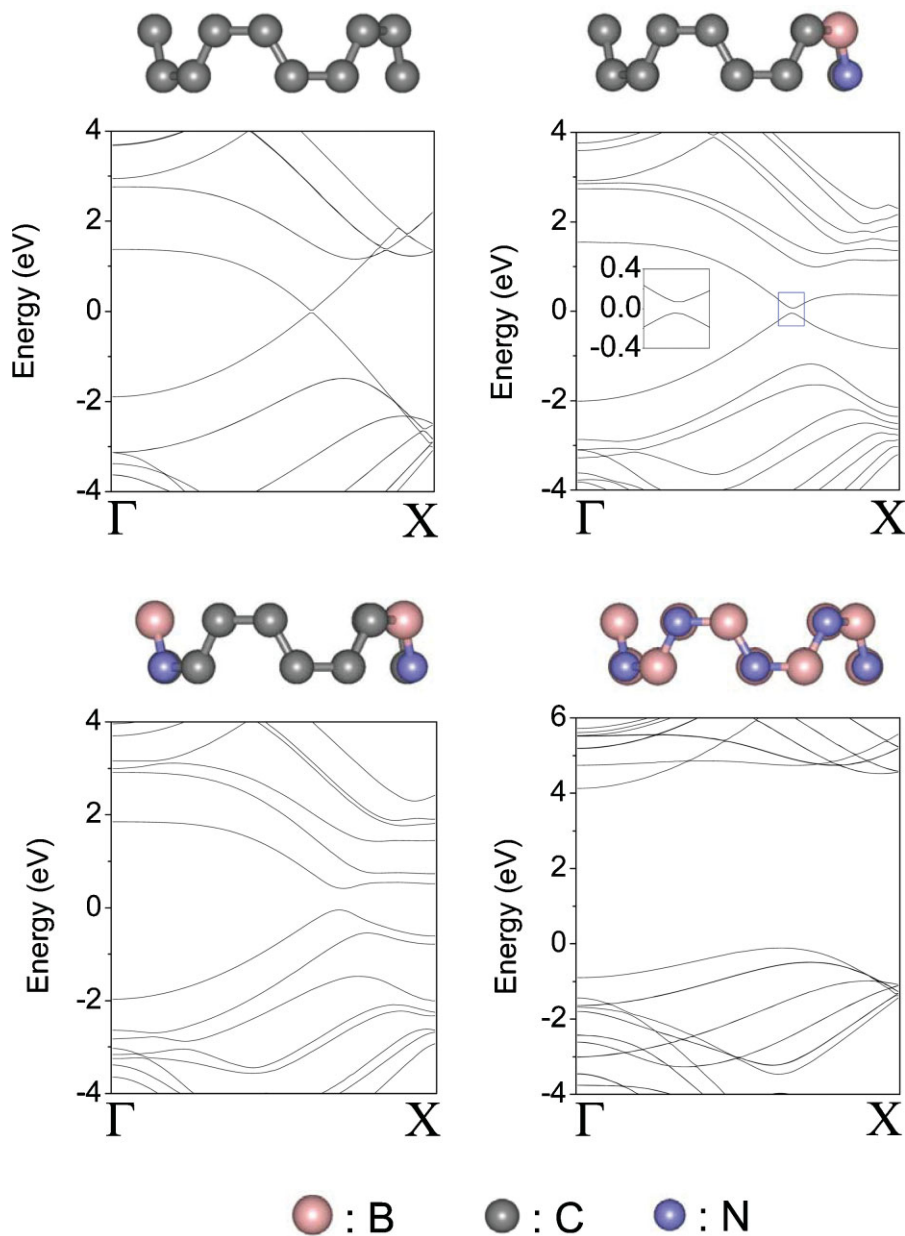


Figure 4. Computed DFT-GGA band structures of a (5,5) BCN-SWNT with a) no B/N atoms (in a pure C nanotube), b) one B/N atom pair per unit cell, c) two B/N atom pairs per unit cell, and d) a pure BN-SWNT. See the structures shown above each band structure. The energy zero in each case is the Fermi level.

Experimental

The synthesis of single-walled BCN nanotubes was achieved by a plasma-assisted HFCVD method. The B/N co-doped C-SWNTs (BCN SWNTs) were grown over the powdery MgO-supported Fe-Mo bimetallic catalyst, by using CH_4 , B_2H_6 , and ethylenediamine vapor as the reactant gases. The filament temperature was 1 650–1 750 °C and the substrate temperature was 800–850 °C.

For fabricating FET devices, the as-grown BCN-SWNTs were first purified and dispersed in dichloroethane solution. The nanotubes were then transferred to an oxidized silicon wafer by spin coating. AFM images were recorded to check the distribution density of the nanotubes on the wafer. The source (S) and drain (D) electrodes with proper size were defined by electron beam lithography to mainly

contact a single nanotube. Ti (2 nm)/Au (30 nm) films were deposited on a wafer for S/D electrodes with a channel distance that ranged from 300 to 800 nm. A Si substrate with an ~70 nm thick SiO_2 surface layer acted as a back gate.

Received: March 26, 2008
Published online: August 27, 2008

- [1] C. Dekker, *Phys. Today* **1999**, 52, 22.
[2] J. Kong, N. R. Franklin, C. Zhou, M. G. Chapline, S. Peng, K. Cho, H. Dai, *Science* **2000**, 287, 622.

- [3] A. Javey, J. Guo, Q. Wang, M. Lundstrom, H. Dai, *Nature* **2003**, *424*, 654.
- [4] Y. Li, D. Mann, M. Rolandi, W. Kim, A. Ural, S. Hung, A. Javey, J. Cao, D. Wang, E. Yenilmez, Q. Wang, J. F. Gibbons, Y. Nishi, H. Dai, *Nano Lett.* **2004**, *4*, 317.
- [5] Z. Chen, X. Du, M.-H. Du, C. D. Rancken, H.-P. Cheng, A. G. Rinzler, *Nano Lett.* **2003**, *3*, 1245.
- [6] Y. Maeda, S. Kimura, M. Kanda, Y. Hirashima, T. Hasegawa, T. Wakahara, Y. Lian, T. Nakahodo, T. Tsuchiya, T. Akasaka, J. Lu, X. W. Zhang, Z. X. Gao, Y. P. Yu, S. Nagase, S. Kazaoui, N. Minami, T. Shimizu, H. Tokumoto, R. Saito, *J. Am. Chem. Soc.* **2005**, *127*, 10287.
- [7] G. Zhang, P. Qi, X. Wang, Y. Lu, X. Li, R. Tu, S. Bangsaruntip, D. Mann, L. Zhang, H. Dai, *Science* **2006**, *314*, 974.
- [8] O. Stephan, P. M. Ajayan, C. Colliex, Ph. Redlich, J. M. Lambert, P. Bernier, P. Lefin, *Science* **1994**, *266*, 1683.
- [9] S. Y. Kim, J. Park, H. C. Choi, J. P. Ahn, J. Q. Hou, H. S. Kang, *J. Am. Chem. Soc.* **2007**, *129*, 1705.
- [10] W. K. Hsu, S. Y. Chu, E. Munoz-Picone, J. L. Boldu, S. Firth, P. Franchi, B. P. Roberts, A. Schilder, H. Terrones, N. Grobert, Y. Q. Zhu, M. Terrones, M. E. McHenry, H. W. Kroto, D. R. M. Walton, *Chem. Phys. Lett.* **2000**, *323*, 572.
- [11] M. Terrones, P. M. Ajayan, F. Banhart, X. Blase, D. L. Carroll, J. C. Charlier, R. Czerw, B. Foley, N. Grobert, R. Kamalakaran, P. Kohler-Redlich, M. Rühle, T. Seeger, H. Terrones, *Appl. Phys. A* **2002**, *74*, 355.
- [12] Y. Miyamoto, A. Rubio, M. L. Cohen, S. G. Louie, *Phys. Rev. B* **1994**, *50*, 4976.
- [13] X. Blase, J.-C. Charlier, A. De Vita, R. Car, *Appl. Phys. Lett.* **1997**, *70*, 197.
- [14] S. Azevedo, R. de Paiva, J. R. Kaschny, *J. Phys.: Condens. Matter* **2006**, *18*, 10 871.
- [15] D. Golberg, Y. Bando, W. Han, K. Kurashima, T. Sato, *Chem. Phys. Lett.* **1999**, *308*, 337.
- [16] W. L. Wang, X. D. Bai, K. H. Liu, Z. Xu, D. Golberg, Y. Bando, E. G. Wang, *J. Am. Chem. Soc.* **2006**, *128*, 6530.
- [17] O. Stephan, P. M. Ajayan, C. Colliex, F. Cyrot-Lackmann, E. Sandre, *Phys. Rev. B* **1996**, *53*, 13 824.
- [18] P. G. Collins, M. S. Arnold, P. Avouris, *Science* **2001**, *292*, 706.
- [19] G. Zhang, P. Qi, X. Wang, Y. Lu, D. Mann, X. Li, H. Dai, *J. Am. Chem. Soc.* **2006**, *128*, 6026.
- [20] G. Drabner, A. Poppe, H. Budzikiewicz, *Int. J. Mass Spectrom. Ion Proc.* **1990**, *97*, 1.
- [21] a) J. P. Perdew, Y. Wang, *Phys. Rev. B* **1992**, *45*, 13 244. b) J. P. Perdew, in *Electronic Structure of Solids*, (Eds: P. Ziesche, H. Eschrig), Akademie Verlag, Berlin **1991**.